

Available online at www.sciencedirect.com

Procedia Engineering 10 (2011) 1823–1828

Engineering
Procedia

ICM11

Macro and micro process modeling of the cutting of carbon fiber reinforced plastics using FEM

R. Rentsch^a, O. Pecat^a and E. Brinksmeier^a *^a IWT Foundation Institute for Materials Science, Badgasteiner Str.3, 28359 Bremen, Germany

Abstract

The most recent developments in the application of carbon fiber reinforced plastics (CFRP), like for passenger aircrafts, wind power stations and hybrid cars, have increased the interest in manufacture of these materials. In this contribution results of two different approaches to the simulation of the cutting process of CFRP will be presented. The macro model is based on continuous but anisotropic material properties with implicitly defined fiber orientation and the micro model on explicit fiber / matrix representation. For verification purposes the simulation results were compared to cutting experiments. Partially the calculated results show very good agreement to experimental findings, e.g. for the material removal mechanism, but the cutting forces and thrust forces are significantly smaller, although tendencies were calculated correctly.

© 2011 Published by Elsevier Ltd. Open access under [CC BY-NC-ND license](https://creativecommons.org/licenses/by-nc-nd/4.0/).
Selection and peer-review under responsibility of ICM11

Keywords: CFRP; cutting simulation; milling; FEM;

1. Introduction

The most recent developments in the fields of passenger aircrafts, wind power stations and hybrid cars have increased the interest in manufacture of parts made of carbon fiber reinforced plastics (CFRP). From the manufacturing point of view, models would be appreciable which are capable of describing the material removal process at CFRP in sufficient detail, so that information regarding the machining forces, the surface integrity and the material removal mechanism can be retrieved [1,2]. Such models would allow to improve the process efficiency and the workpiece quality on basis of numerical parameter studies and tool design studies. In the literature already several cutting process simulations based on FEM modeling for fiber reinforced plastics (FRP) and CFRP are published [3,4,5]. The conclusion of the

* R. Rentsch. Tel.: +49-421-218-5390; fax: +49-421-218-3272.
E-mail address: rentsch@lfm.uni-bremen.de.

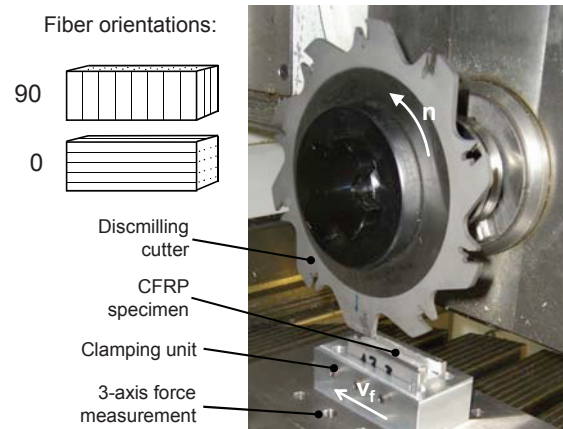


Fig. 1. Experimental setup for milling a slot in CFRP specimen with fiber orientation 0° and 90° (relative to cutting direction)

literature review and the requirements of the experimental setup led to the selection of the employed software as well as the model development described below. Two different modeling approaches to the cutting process simulation of CFRP have been developed: a macroscopic type with continuous but anisotropic material properties, because of the fiber orientation, and a microscopic model with explicit fiber / matrix representation. For verification purposes the simulation results will be discussed in comparison to cutting experiments, which will be presented first.

2. Cutting experiments

Cutting experiments have been carried out using a disc milling cutter with a diameter of 160 mm and one carbide insert cutting slots in CFRP specimens (cf. figure 1). The cutting radius was about 35 microns and the face angle -7° . Depending on the fiber orientation, the cutting direction was either along horizontally lying fibers (0°) or across vertically oriented fibers (90°) applying dry up-cut milling conditions. The experiments were carried out at a cutting speed v_c of 100 m/min, a depth of cut a_c of 0.6 mm and a feed per tooth f_z of 0.1mm/rev. Besides cutting force measurements the surfaces were analyzed on basis of micrographs. Figure 2 shows the fiber structure below surfaces at the bottom of milled slots of two specimens with different fiber orientation at otherwise identical milling parameters. The milled surfaces of the specimens with vertically oriented fibers (90° , figure 2 left) are somewhat rougher than those with

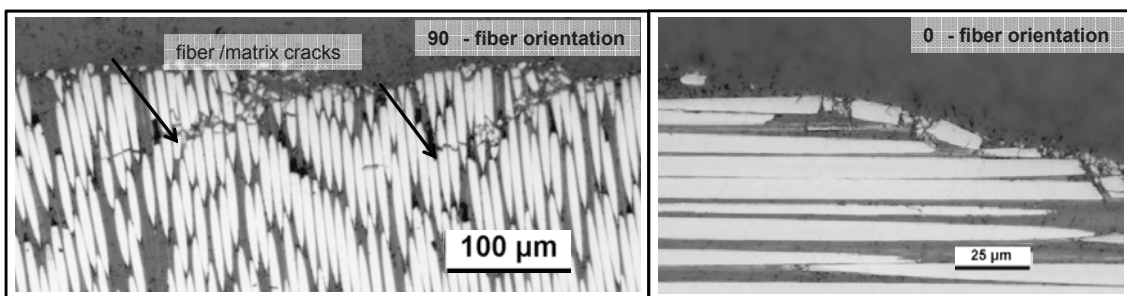


Fig. 2. Fiber / matrix microstructures in cutting direction (from right to left) at bottom of milled slots in CFRP specimens with fiber orientation 90° (left figure) and 0° (right figure)

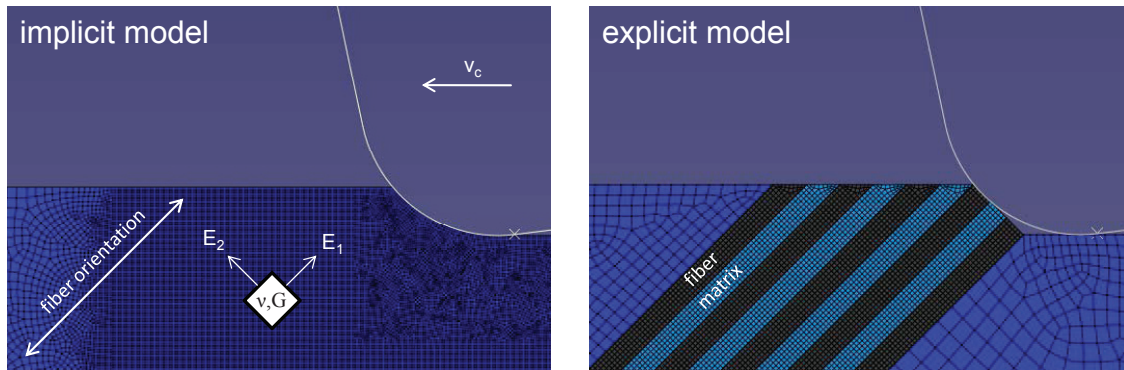


Fig. 3. Setups of the implicit macroscopic (left) and the explicit microscopic model (right) for the CFRP cutting simulation

horizontally lying fibers (0°). While the specimens with 90° fiber orientation show cracks extending frequently from the milled surface at an angle of 18° into the material at intervals of about 200 microns, the surfaces of the specimens with horizontal fibers (0° , figure 2 right) show no cracks and are very smooth. The micrographs further show that the fiber structure of the specimens with 0° fiber orientation is hardly altered at all, usually only the very outer fibers are broken into pieces.

3. Design of the cutting process models

The models were designed two dimensional in a so-called orthogonal cutting setup considering a rigid cutting edge (contour lines in figure 3) engaging with the CFRP specimens. All values were chosen according to chapter 2, additionally the friction coefficient was set to 0.3. The cutting conditions result in a maximum chip thickness h_{max} of 12.5 microns, which was used as engagement depth in the models. For the cutting process simulation of CFRP material two different approaches were developed: a macroscopic model, which is based on continuous but anisotropic material properties with implicitly defined fiber orientation, and a microscopic model with explicit fiber / matrix representation (cf. figure 3). While the implicit macroscopic model focuses on average process information, like cutting forces and workpiece shape, the explicit microscopic model allows to study the cutting mechanism itself und details of the local fiber and matrix damage. The employed software is the FEM program ABAQUS using element type CPS4R. For the cutting process simulation the progressive damage model by Hashin [6] was considered (cf. figure 4). At increasing load the stress of the fibers as well as the matrix elements

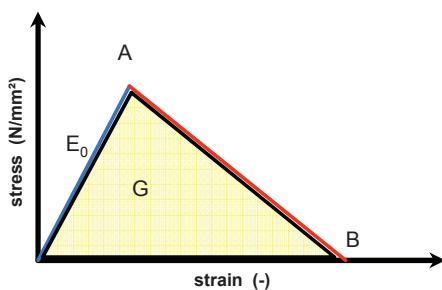


Fig. 4. Material behaviour at progressive damage

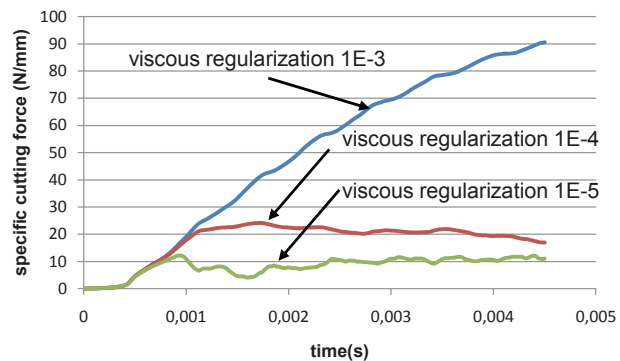


Fig. 5. Influence of viscose regularisation on the cutting force

Table 1. Material data for the implicit macroscopic model (^k Calculated according to [7] using data from [8]; ^l from [3])

Mechanical properties	CFRP	Mechanical properties	CFRP
E-Modulus E_{11} (MPa)	116000 ^k	Shear strength S^I (MPa)	79 ^l
E-Modulus E_{22} (MPa)	8500 ^k	Shear strength S^T (MPa)	79 ^l
Shear modulus G_{12} (MPa)	3260 ^k	Fracture energy (tensile) G_{LT}	0.01
Poisson ratio ν_{12} (-)	0.32 ^k	Fracture energy (compressive) G_{LC}	0.005
Tensile strength X^T (MPa)	1950 ^l	Fracture energy (transv.,tensile) G_{TT}	0.0009
Compressive strength X^C (MPa)	1480 ^l	Fracture energy (transv.,compr.) G_{TC}	0.006
Transv. Tensile strength Y^T (MPa)	48 ^l	Hashin coefficient α	1
Transv. Compressive strength Y^C (MPa)	200 ^l	Viscose regularization VR (all)	1E-7
Density ρ (g/cm ³)	1.47		

follows from the origin to point A. As a material would be damaged beyond its maximum strength, the elements progressively loose in strength without recovering when being strained beyond point A. In point B the material can be considered being broken. The converted energy of this damage process is the fracture energy G , which is equivalent to the area of the triangle in figure 4. The necessary data for the progressive damage model of the CFRP for all directions are listed in table 1. The material data were retrieved from the fiber and matrix manufacturers [8] or from literature [3, 5, 9, 10]. It was found that a program parameter of ABAQUS, the so-called viscous regularization has a significant influence (via the cutting speed) on the calculated cutting force (cf. figure 5). This unwanted effect could be suppressed by choosing a suitably small number (cf. table 1). The microscopic model contains only a few explicit fibers because of the numerical expense and the rapid model degradation soon after damage initiation due to the tool impact. Here fiber and matrix were modeled with the element type CPS4R and the interface between them with element type COH2D4 using data from [5].

4. Cutting and modeling results

Figure 6 shows the measured and calculated process forces during a single tool / workpiece contact. Because of the up-cutting condition the experimental forces gradually increase from the beginning to the

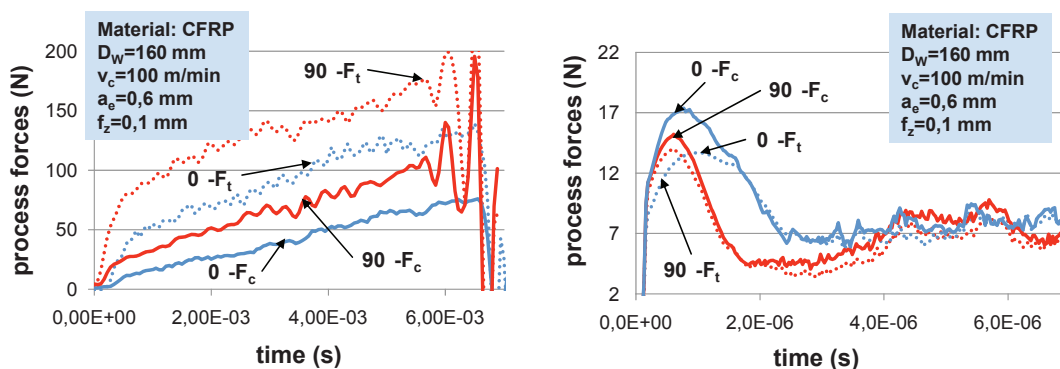


Fig. 6. Cutting and thrust forces for one cutting edge contact to unidirectional CFRP with 0° and 90° fiber orientation: (left) experimental measurements and (right) calculated data of the macroscopic model; (F_c –cutting force, F_t – thrust force, D_w – diameter of milling cutter, v_c – cutting speed, a_e –depth of cut, f_z – feed per tooth and revolution)

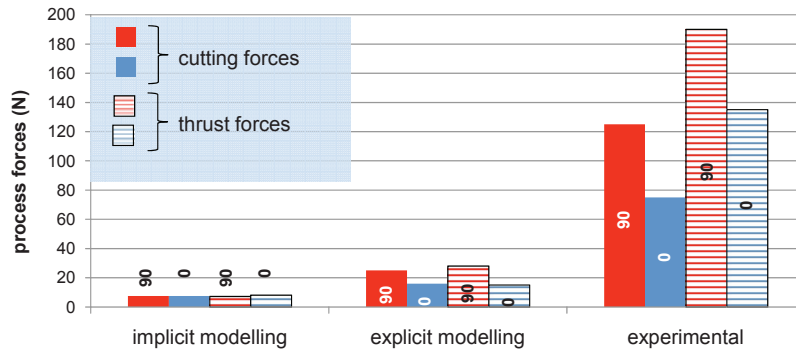


Fig. 7. Comparison of calculated and measured cutting and thrust forces for 0° and 90° fiber orientation

end of contact, where the maximum chip thickness is reached. Here the 90° fiber orientation shows a strong dynamic response in the forces, presumably due fiber fracture related process instabilities. For both fiber orientations the cutting forces F_c are lower than the thrust forces F_t . In comparison the calculated forces are significantly lower than the measured ones (cf. Figure 6). The different course of the calculated forces results from the model starting condition, in which a head-on collision determines the initial course. Hence only the course of the forces after the initial conditions was used in this analysis. Figure 7 shows averaged forces for a depth of cut of 12.5 microns (max. chip thickness). For the macroscopic implicit model as well as for the microscopic explicit model the forces are much lower than measured in experiment. The forces of the microscopic explicit model show somewhat larger values than the macroscopic implicit one and this approach reflects a comparable tendency to the experimental forces.

As the weaker CFRP component the matrix plays an important role in the material removal process as well as regarding the composite failure mode. Figure 8 shows the calculated matrix damage distributions.

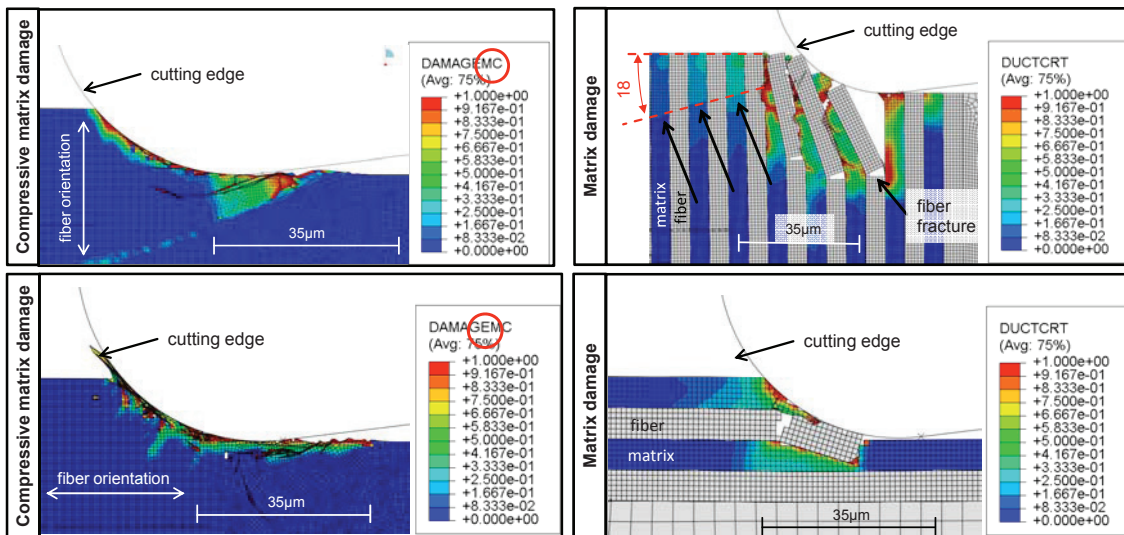


Fig. 8. Calculated matrix damage distributions in the macroscopic model (left) and the microscopic model (right): top row for a fiber orientation of 90° and bottom row for 0° fiber orientation.

The macroscopic model (Fig. 8 left) describes the load and the failure mode for both fiber orientations (0° and 90°) quite well. For the 90° fiber orientation a deep running matrix damage can be observed at about the same angle as for the corresponding experiment (cf. Fig. 2 left), whereas the 0° fiber orientation doesn't develop any deeper damage as observed in the experiment as well. The microscopic model provides further insight into the underlying material removal mechanisms as well as related damage modes (cf. Fig. 8 right). At 90° fiber orientation the matrix between the fibers is loaded to the point of total damage (cf. to point B in Fig.4) upon these matrix elements are deleted. As consequence the fibers bending more and fracture significantly below the cutting plane. It is interesting to notice that the development of the deep running matrix failure (at about 18°) can already be detected here in the compressive stress distribution ahead of the cutting edge (Fig.8, upper right). The simulation for the 0° fiber orientation shows a similar effect regarding the matrix behavior. The cutting edge compresses matrix and fibers upon which, again the matrix exceeds its maximum strength first and its elements are deleted by the program. The fibers are also break due to a bending load. The fractured 0° fiber segment in the microscopic model (Fig. 8 lower right) resembles very much the found fragments of the corresponding experiment (cf. Fig.2 right).

5. Conclusions

A macroscopic CFRP model, based on continuous but anisotropic material properties with implicit fiber orientation, and a microscopic model with explicit fiber / matrix representation were developed for the simulation of the material removal process. Partially the calculated results show very good agreement to experimental findings, e.g. for the material removal mechanism, but the calculated cutting forces and thrust forces are significantly smaller than the experimental ones, although tendencies were calculated correctly in case of the explicit fiber / matrix model. Despite the close resemblance of the apparent material removal mechanisms and the fiber / matrix failure mode, the discrepancy of the calculated forces from experimental ones is assumed to result from the progressive damage model by Hashin in both models, for the implicit as well as for the explicit fiber / matrix representation. When exceeding the compressive strength of a CFRP component in the experiment it must yield, but it can still carry a compressive load as it is still physically present in the tool / workpiece contact. However when the finite elements reach the total damage state of the progressive damage model, the elements in the FEM model cannot carry load anymore and will be deleted. Accordingly lower cutting forces will be calculated.

References

- [1] Ferreira JR, Coppini NL, Miranda GWA. Machining optimisation in carbon fibre reinforced composite materials. *Journal of Materials Processing Technology*, Vol. 92, 1999, p.135-140.
- [2] Teti R. Machining of Composite Materials. *CIRP Annals – Manufacturing Technology*, Vol. 51, 2002, p.611-34.
- [3] Santiuste C, Soldani X, Henar M. Machining FEM model of long fiber composites for aeronautical components. *Composite Structures* 92, 2010, p. 691–8.
- [4] Venu Gopala Rao G, Mahajan P, Bhatnagar N. Machining of UD-GFRP composites chip formation mechanism. *Composites Science and Technology*, Vol. 67, 2007, p.2271–81.
- [5] Venu Gopala Rao G, Mahajan P, Bhatnagar N. Micro-mechanical modeling of machining of FRP composites – Cutting force analysis, *Composites Science and Technology*, Vol. 67, 2007, p.579–93.
- [6] Hashin Z. Failure Criteria for Unidirectional Fiber Composites. *Journal of Applied Mechanics*, Vol 47, 1980, p.329–34.
- [7] Schürmann H. *Konstruieren mit Faser-Kunststoff Verbunden (Designing with FRP)*. Springer Verlag, Berlin, 2007.
- [8] Toho Tenax, manufacturer of fiber type HTS; epoxy matrix material by Hexion corporation; explicit model: the fiber fracture energy parameters were set to: $GLT = 0.04$, $GLC = 0.01$, $GTT = 0.003$, $GTC = 0.13$, $\alpha = 0$, $VR = 0$;
- [9] Gilat A, Goldberg RK, Roberts GD. Strain Rate Sensitivity of Epoxy Resin in Tensile and Shear Loading. *Journal of Aerospace Engineering*, Vol. 20, 2005, p.75-89.
- [10] Zheng X. Nonlinear Strain Rate Dependent Composite Model. *J. of Aerospace Engineering*, Vol. 21, 2006, p.140-51.